Weldability and Toughness Evaluation of Pressure Vessel Quality Steel Using the Shielded Metal Arc Welding (SMAW) Process

R. Datta, D. Mukerjee and S. Mishra

(Submitted 5 November 1997; in revised form 8 May 1998)

The present study was carried out to assess the weldability properties of ASTM A 537 Cl. 1 pressure-vessel quality steel using the shielded metal arc welding (SMAW) process. Implant and elastic restraint cracking (ERC) tests were conducted under different welding conditions to determine the cold cracking susceptibility of the steel. The static fatigue limit values determined for the implant test indicate adequate resistance to cold cracking even with unbaked electrodes. The ERC test, however, established the necessity to rebake the electrodes before use. Lamellar tearing tests carried out using full-thickness plates under three welding conditions showed no incidence of lamellar tearing upon visual examination, ultrasonic inspection, and four-section macroexamination. Lamellar tearing tests were repeated using machined plates, such that the central segregated band located at the midthickness of the plate corresponded to the heat-affected zone (HAZ) of the weld. Only in one (no rebake, heat input: 14.2 kJ cm^{-1}, weld restraint load: 42 kg mm^{-2}) of the eight samples tested was lamellar tearing observed. This was probably accentuated due to the combined effects of the presence of localized pockets of a hard phase (bainite) and a high hydrogen level (unbaked electrodes) in the weld joint. Optimal welding conditions were formulated based on the above tests. The weld joint was subjected to extensive tests and found to exhibit excellent strength (tensile strength: 56.8 kg mm^{-2}, or 557 MPa), and low temperature impact toughness (7.4 and 4.5 kg-m at –20 °C for weld metal, WM, and HAZ) properties. Crack tip opening displacement tests carried out for the WM and HAZ resulted in δ_m values 0.36 and 0.27 mm, respectively, which indicates adequate resistance to brittle fracture.

Keywords cold cracking, crack tip opening displacement, impact toughness, lamellar tearing, restraint intensity, sheilded metal arc welding

1. Introduction

Pressure vessel quality steel conforming to ASTM A 537 Cl. 1 specification is extensively used for the manufacture of containers, tankers, and spheres for the storage of oil and natural gas. The steel provides adequate strength levels of yield strength (YS) 35 kg mm^{-2}, tensile strength (TS) 50 to 63 kg mm^{-2}), good low temperature impact toughness with Charpy impact energy (CIE) 20 J min at –20 °C), and a guarantee against ultrasonic defects. The steel was successfully produced at the Bhilai Steel Plant through the basic oxygen furnace (BOF), vacuum arc degassing (VAD), concast route and rolled into plates in thicknesses ranging from 8 to 36 mm. The alloy chemistry designed and the processing parameters adopted have been described elsewhere (Ref 1, 2). More than 20,000 tons of this steel have been successfully produced and used for various end uses.

Welding forms an important processing step during the conversion of these input steel plates to the end product. The life and performance of the end product depends largely on the soundness and integrity of the weld joint. In turn, the integrity of the weld joint is strongly influenced by the microstructure, carbon equivalent (CE), hydrogen content, weld cooling rate, and lamellar tearing susceptibility. The above factors, singly or in combination, can lead to the premature failure of the weld joint.

The resistance of a steel to two basic types of weld cracking (cold and hot), forms the basis of steel weldability assessment (Ref 3-6). Cold cracking, also commonly referred to as hydrogen-induced cracking (HIC) or delayed cracking, is related to the contamination of the weld microstructure with hydrogen. In addition to the hydrogen content and the CE, the microstructures of the weld metal (WM) and the heat affected zone (HAZ) strongly influence the cold cracking susceptibility. A martensitic microstructure has the highest susceptibility to HIC, followed by bainite and acicular ferrite. A ferrite-pearlite structure is the least susceptible to hydrogen embrittlement.

In the present work, an attempt was made to assess the resistance of ASTM A 537 Cl. 1 steel to cold cracking using the shielded metal arc welding (SMAW) process. Additionally, the lamellar tearing resistance of the steel under different welding conditions was evaluated. Based on the above work, a judicious choice of appropriate welding parameters and consumables was made to ensure a safe and sound weld joint.

2. Experimental

2.1 Steelmaking and Rolling

Steel was made in a 130 T BOF and then transferred to an argon rinsing station where it was treated for 3 to 7 min at an argon flow rate of 35 to 45 m^3/h to ensure homogenization, the

R. Datta, D. Mukerjee, and **S. Mishra,** Steel Authority of India Ltd., Research and Development Centre for Iron & Steel, Ranchi 834002, Bihar, India.

floating out of inclusions, and uniformity of metal temperature in the ladle. The steel was next treated in a 110 T VAD unit. In addition to improving cleanliness, the VAD helped achieve effective desulfurization and fine tuning of composition. A sulfur level of less than 0.01wt% was achieved consistently through this process. The steel was continuously cast into 200 by 1500 mm or 250 by 1500 mm slabs, depending on the final plate thickness. The slabs were reheated to 1250 ± 10 °C and conventionally rolled in a modern 3600 mm plate mill. The rolling was performed following a longitudinal-transverse scheme in the roughing stand and a longitudinal scheme in the finishing stand. A reduction of 60 to 65% was employed during finish rolling to facilitate elongation of the austenite grains, leading to a higher austenite interfacial area (S_V) and a finer grain size on cooling. The finish rolling temperature was maintained within 850 to 880 °C. The plates were water spray cooled on the run-out table to a temperature of 700 to 720 °C, followed by air cooling. Typical chemical composition and mechanical properties of ASTM A 537 Cl. 1 plates are shown in Table 1.

2.2 Microscopy

Longitudinal sections of the plates were polished and etched with 2% nital for optical microscopy examination. Analysis of elemental segregation at the midthickness of the plates was carried out using an electron probe microanalyzer (EPMA). The volume fraction of pearlite was determined using a quantitative image analyzer.

2.3 Mechanical Property Evaluation

Tensile samples were prepared as per ASTM 10 (PA-370) specification and tested on a 10 ton static universal testing machine at a strain rate of $6.6 \times 10^{-4} s^{-1}$. Standard Charpy V-notch samples were prepared and tested at –20 °C for Charpy impact energy (CIE). The temperature rise during testing was within 2 °C. Crack-tip opening displacement (CTOD) tests were carried out as per BS 7448 Part 1 (1991) specification.

2.4 Weldability

The cold cracking susceptibility of the weld joint was determined by the implant test. Standard procedure for conducting this test has been specified by the International Institute of Welding (IIW) in 1973 (Ref 7). Here, one end of a 6 mm diameter cylindrical specimen was inserted with a sliding fit into a hole bored in a plate called the "host plate." The other end of the specimen was threaded to facilitate application of load through a loading bar. A weld bead was lain under conditions of investigation on the host plate across the implant specimen. The set up was allowed to cool to a temperature, usually 100 °C, before a predetermined static tensile load was applied to the specimen by a "constant loading system" until failure occurred or 24 h lapsed, whichever was earlier. The maximum stress that the weld joint could withstand without failure was determined by testing at different stress levels and known as the static fatigue limit (SFL).

Most welded structures are subject to the combined effects of welding as well as restraining stresses. The elastic restraint test is designed to combine both types of stresses and simulate a situation that is actually experienced in real life situations. Here, two plate specimens were clamped rigidly into a clamping frame with high strength bolts. The material and geometry of the frame was chosen so that it behaved elastically at all levels of reaction stress. In the test, different levels of restraint intensities were generated depending upon the restraining frames and welding conditions. Weld cracks occurred when the restraint intensity (K) imposed was higher than a critical level, known as the critical restraint intensity (K_{cr}). The K_{cr} value was determined under different welding conditions.

The lamellar tearing test comprised welding a cantilever to a rigid vertical test plate by depositing a multi-run weld in a 45° bevel groove while maintaining a constant level of through-thickness stress called the weld restraint load (WRL). The test plates were allowed to bear load for 24 h to allow HIC cracks to initiate and trigger lamellar tearing.

Table 1a Typical chemical composition of ASTM A 537 Cl. 1 grade steel

Chemistry, wt% C	Mn	Si	Al	S	P
0.19-0.23	1.30-1.35	0.25-0.35	0.02-0.03	0.01 max	0.015 max

Table 1b Typical mechanical properties of ASTM A 537 Cl. 1 grade steel

Yield strength, kg mm^{-2}	Ultimate tensile strength, kg mm^{-2}	Elongation, %	Charpy V-notch, kg-m –20 °C	Bend
36-39	58-61	25-28	8-12	2 T

Table 2 Static fatigue limit (SFL) values of ASTM A 537 Cl. 1 plates under different welding conditions

Type of electrode	Welding Conditions			Static fatigue limit, kg mm^{-2}
	Rebake	Preheat, °C	Heat input, (kJ cm^{-1})	
AWS E 7018-1	Nil	Nil	10.5	46.6
	300 °C 1 h	Nil	10.5	45.8
	350 °C 2 h	Nil	10.5	52.0

3. Results and Discussion

3.1 Implant Test

The implant test results on a 13 mm thick plate are in Table 2. The welding was carried out using AWS A 5.1 E 7018-1 electrodes of 3.15 mm diameter and 10.5 kJ cm^{-1} heat input. The SFL values obtained for the three welding conditions, namely, no rebake, partial rebake (300 °C for 1 h) and full rebake (350 °C for 2 h) were 46.6, 45.8, and 52.0 kg mm^{-2} respectively. These values were well above the minimum specified yield strength (MSYS) of the steel (35 kg mm^{-2}). Figure 1 shows a SFL plot for the steel using no preheat, no rebaking of electrodes and heat input (HI) of 10.5 kJ cm^{-1}. It may be noted that the SFL value was determined on the basis of a series of stepwise tests carried out at different stress levels, and the symbols (◆) and (✧) indicate failure and success respectively. A high SFL value of 46.6 kg/mm^{-2} indicates adequate cold cracking resistance of the weld joint, even with unbaked electrodes (and a relatively high hydrogen level).

The type of heat flow for the implant weldability test (heat input: 10.5 kJ cm^{-1}, plate thickness: 13 mm) as well as the butt welding test using the SMAW process, corresponded to three-dimensional flow. The corresponding cooling time from 800 to 500 °C ($\Delta t_{8/5}$) worked out to be 4.6 and 4.5 s for the implant and butt welding tests respectively. Thus, it may be inferred that the welding thermal cycle for the implant and butt weld tests were similar.

3.2 Elastic Restraint Cracking (ERC)

The sensitivity of cracking of the root layer in butt welding was tested by imposing different levels of restraint intensities, varying from 630 to 4360 kg/mm^2. Figure 2 shows a photomacrograph of a sound weld joint specimen subjected to a restraint intensity (K) of 3260 kg/mm^2 using fully baked electrodes. When the ERC test was repeated using a restraint intensity of 3820 kg/mm^2, cracks were observed upon visual examination. The critical restraint intensity (K_{cr}), determined as the mean of the two values (3260 and 3820), was found to be 3540 kg/mm^2 in this case. The welding conditions used and the critical restraint intensities (K_{cr}) obtained are summarized in Table 3. The K_{cr} values obtained under no rebake, partial rebake and full rebake conditions were 990, 3540, and 3540 kg/mm^2, respectively. If one compares these values with the actual restraint intensities experienced for different structural applications (Table 4), it may be concluded that baking of the electrodes (K_{cr}: 3540 kg/mm^2) is necessary to provide adequate protection to the weld joints for most end uses.

3.3 Lamellar Tearing Resistance

Under certain conditions of welding, a low through-thickness ductility may contribute to the formation of separations lying beneath the weld and parallel to the plane of the plate. These separations, termed lamellar tearing, are caused by stresses generated in the through-thickness direction resulting from weld contraction, high surface area of planar inclusions, high hydrogen level, and faulty weld joint design.

Lamellar tearing tests were conducted simulating the normal conditions of fabrication involving fillet welds. Tests conducted using full-thickness specimens, three welding conditions (no rebake, partial rebake, and full rebake), three electrode diameters (3.15, 5.0, and 6.3 mm), and a weld restraint load of 42 to 44 kg mm^{-2} showed no incidence of cracks upon visual, ultrasonic, or macroexamination. The results indicate good lamellar tearing resistance of the weld joint.

Table 3 Elastic resistant cracking test results under different welding conditions

Type of electrodes	Welding conditions			Critical restraint intensity, K_{cr}, kg/mm^2
	Rebake	Preheat, °C	Heat input, (kJ cm^{-1})	
AWS E 7018-1	Nil	Nil	12.0	990
	250 °C 1 h	Nil	12.0	3540
	350 °C 2 h	Nil	12.0	3540

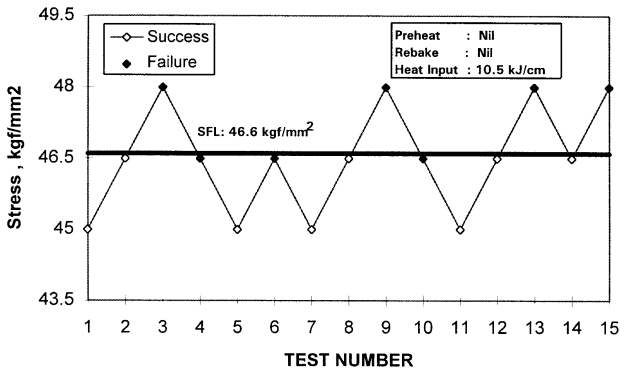

Fig. 1 Static fatigue limit plot for ASTM A 537 Cl. 1 steel using no preheat, no rebake of electrodes, and a heat input of 10.5 kJ cm^{-1}

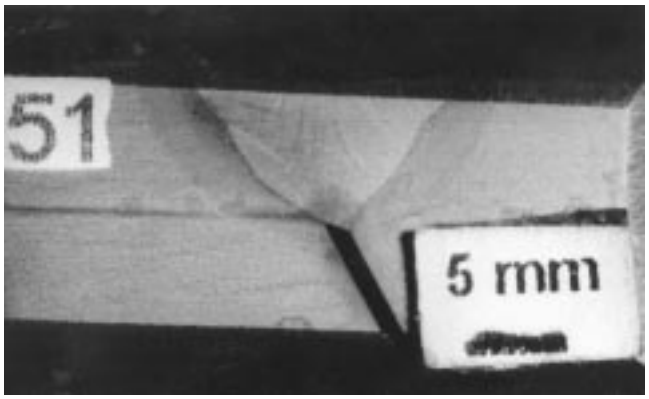

Fig. 2 Photomacrograph of a sound weld joint using fully baked electrodes and a restraint intensity of 3260 kg mm^{-2}

Centerline segregation, a common quality problem associated with concast slabs and plates, adversely affected the through-thickness ductility of the steel. Electron probe microanalyzer studies were conducted to identify the elements responsible for centerline segregation. Figure 3(a) shows a scanning electron image (SEI) taken from the midthickness of a plate exhibiting a segregated zone (band) surrounded by the matrix. Figure 3(b) and (c) shows x-ray line profiles of C, S, P, and Mn respectively along the line of analysis. It is clearly evident from the analysis that C and Mn have a strong tendency to segregate. The segregation of C and Mn not only leads to a higher pearlite content (~80%) at the core of the plate (see Fig. 4), but also leads to the localized formation of a hard phase, namely, bainite or martensite. These bainite/martensite pockets are preferential sites for crack nucleation due to their poor ductility and toughness properties. This is directly corroborated by Figure 5 which shows an optical photomicrograph taken from the midthickness of a 36 mm thick plate showing localized pockets of bainite and initiation of cracks within them.

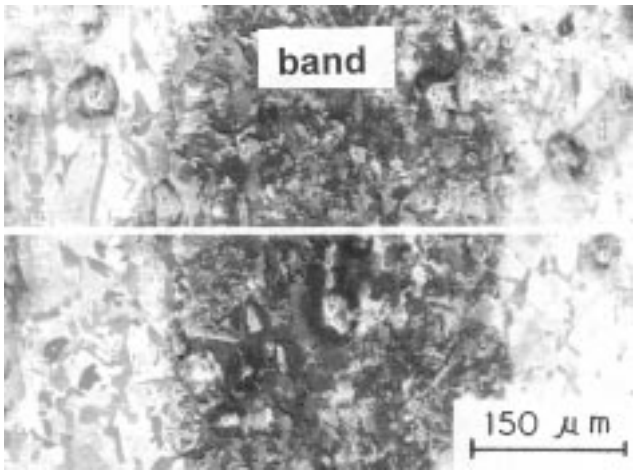

(a)

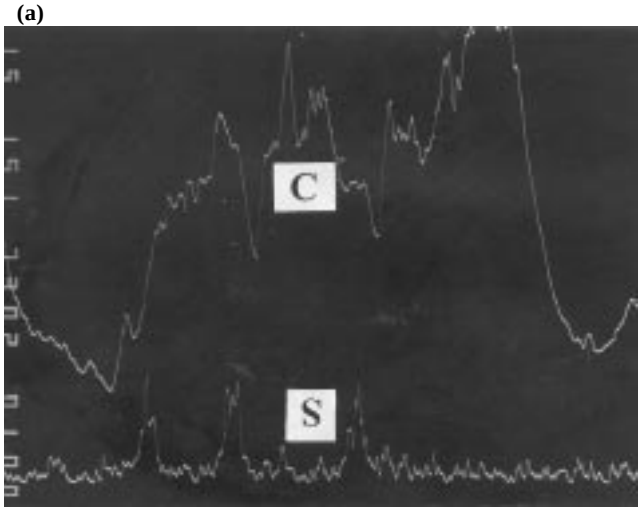

(b)

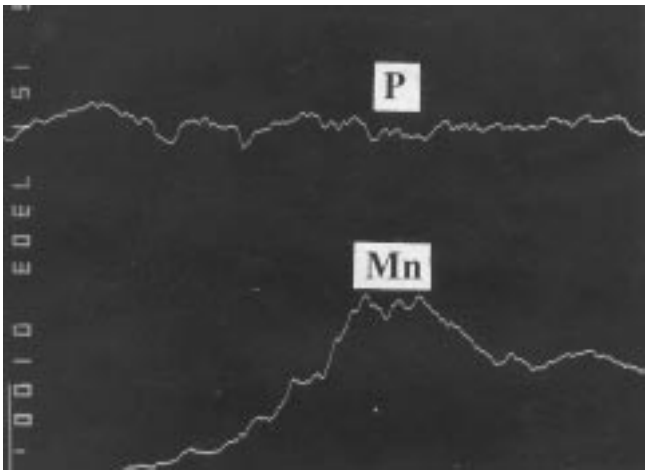

(c)

Fig. 3 (a) Scanning electron image of a sample taken from the midthickness of a 36 mm plate. (b) Line profiles of C and S. (c) Line profiles of P and Mn

In view of the strong influence of centerline segregation on the susceptibility to weld cracking and hydrogen-induced crack (HIC) formation (Ref. 8, 9), the lamellar tearing tests were repeated using machined specimens, such that the centerline segregated zone corresponded to the HAZ. The 13 mm thick plate was machined down to 9.5 mm thickness. This positioned the segregation line at a distance of 3 mm from the plate surface, corresponding to the HAZ of the weld. Out of eight plate specimens tested under different welding conditions (electrode diameter: 3.15, 5, and 6.3 mm; baking condition: no rebake and partial rebake) and a WRL of 42 kg mm^{-2}, only one specimen (unbaked electrode HI: 14.2 kJ cm^{-1}) was observed to exhibit lamellar tearing upon visual, ultrasonic and macroexamination. Figure 6 shows an optical photomicrograph of the failed specimen showing the propagation of lamellar tearing in a stepwise fashion at a region slightly away from the HAZ. The lamellar tearing was probably triggered by a cold crack due to the combined effects of a higher hydrogen level (unbaked electrode) and a hard microstructure (bainite) at the weld joint.

3.4 Weld Joint Properties

Based on the results of the weldability tests described above, the butt welding procedure and welding conditions chosen were: rebake, 350 °C for 2 h; preheat, nil; interpass temperature, 250 °C max; number of passes, 8; heat input, 10 to 12 kJ cm^{-1} for 3.15 mm and 17 to 19 kJ cm^{-1} for 4 mm electrode diameter; and welding speed, 120 to 140 mm min^{-1}. Butt welding was carried out and the weld was subjected to

Table 4 Restraint intensities for different structural applications

Applications	Location	Thickness, mm	Restraint intensity (*K*), kg/mm^2
Ship	Transverse bulk head	16	1640
	Longitudinal bulk head	14	1260
	Bottom shell	28	780
	Upper deck	32	1280
Bridge	Diaphragm and web plate	19-38	200
	Diaphragm and flange plate	40-60	1800
Building frame	Building column construction	28	1090

microstructural examination. Figure 7 (a) and (b) show optical micrographs of the weld zone and HAZ. The weld zone revealed a predominantly acicular ferrite microstructure with islands of proeutectoid ferrite at prior austenite grain boundaries (Fig. 7a). The HAZ microstructure, on the other hand, revealed a typical bainitic structure (Fig. 7b).

Various tests were conducted to characterize the weld joint properties. The transverse tensile strength of the weld joint was

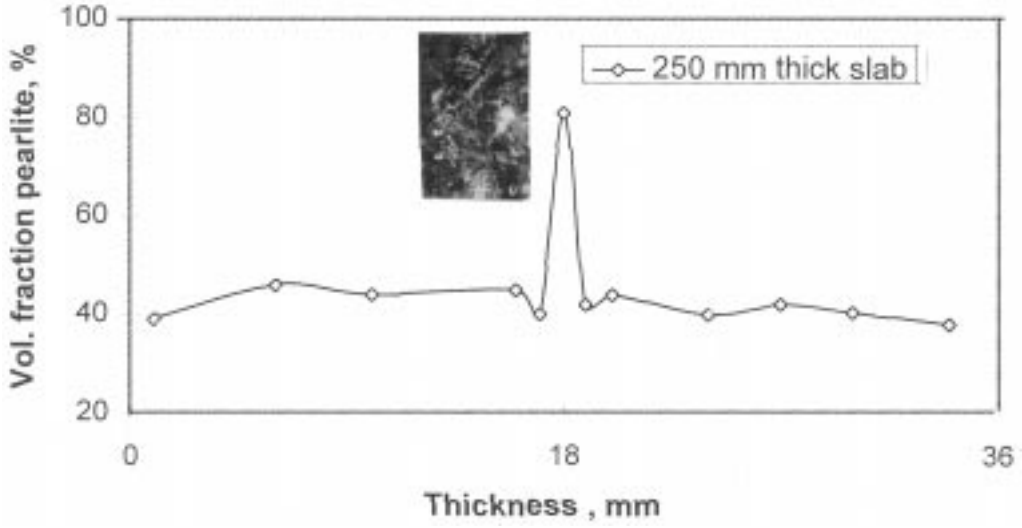

Fig. 4 Variation of pearlite volume fraction across the thickness of a 36 mm plate

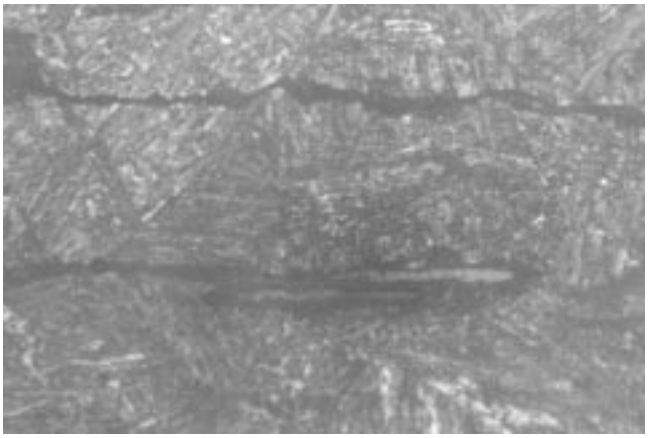

Fig. 5 Optical micrograph showing evidence of internal cracks within localized bainitic pockets at the midthickness of a plate

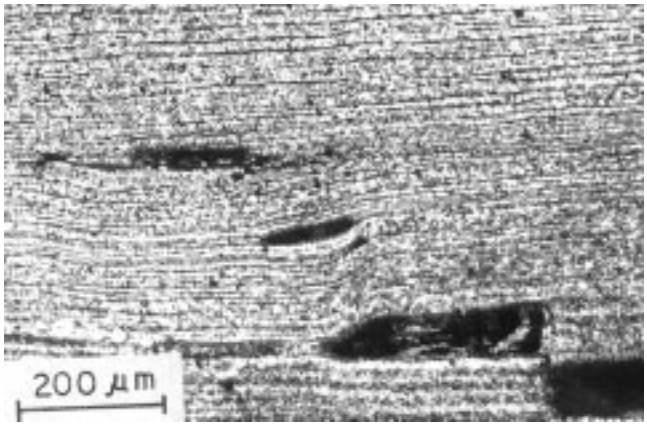

Fig. 6 Optical micrograph showing propagation of lamellar tearing in a stepwise fashion at a region slightly away from the HAZ

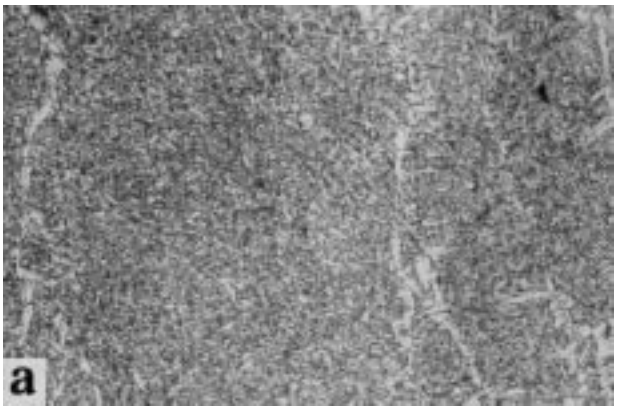

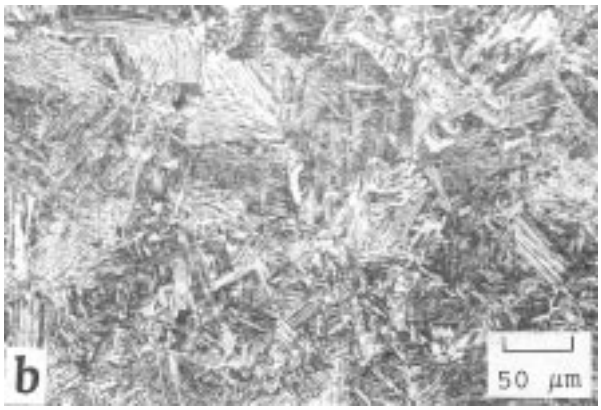

Fig. 7 Optical micrograph of (a) weld metal and (b) HAZ exhibiting acicular ferrite and bainite microstructures respectively

56.8 kg mm^{-2}, comparable to the typical strength level of the parent metal (58 to 61 kg mm^{-2}, Table 1b) and significantly higher than the minimum specified tensile strength (MSTS) of 50.0 kg mm^{-2}. The Charpy impact test results are presented in Fig. 8. The impact energy levels for the parent metal (PM) and WM are significantly higher than that of the HAZ at 25, 0, and –20 °C. This means that the HAZ is the likely zone for crack initiation and propagation. However, it may be noted that the impact energy levels determined for the PM, WM and HAZ fulfill the minimum specified requirement of 2 kg-m at –20 °C for ASTM A 537 Cl. 1 steel. Crack tip opening displacement (CTOD) tests were carried out for the PM, WM, and HAZ. The CTOD (δ_m) values for the WM (0.36 mm) and HAZ (0.27 mm) were higher than values for the PM (0.09 mm), which was quite low. It can be concluded that the WM and HAZ possess moderate resistance to brittle fracture. Figure 9 depicts hardness values across the weld joint. The hardness varied within a range from 153 to 274 HV. The hardness range of PM, WM and HAZ were: PM, 153-186; HAZ, 191-274; and WM, 176-238 HV. A higher hardness level in the HAZ reflects the presence of a hard microstructure, which was bainite in the present case. It also indicates a lower impact toughness value for the HAZ as compared to the PM and WM. This agrees very well with the impact test results described earlier. However, the low CTOD value obtained for the PM cannot be explained in terms of the impact and hardness test results.

Table 5 Tensile shear test results for five weld joint configurations

Welding condition: preheat, nil; rebake, 350 °C 2 h

Type of joint	Tensile strength, kg/mm^2	Position of fracture
Single lap	52.0	PM
Double lap	51.1	PM
Angular butt joint	51.0	HAZ
Cruciform fillet with prepared edge	52.0	PM
Cruciform fillet without edge preparation	53.0	PM

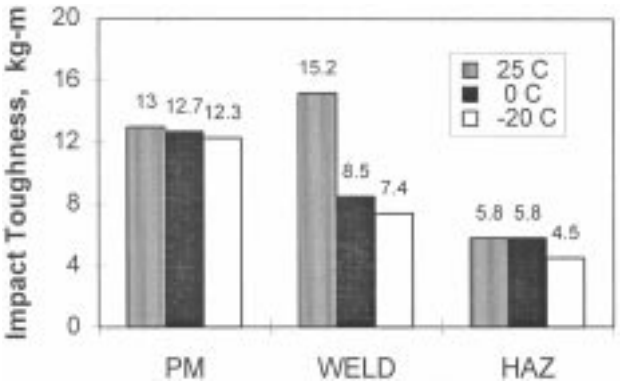

Fig. 8 Comparison of Charpy impact energies of parent metal, weld metal and HAZ at 25, 0 and –20 °C

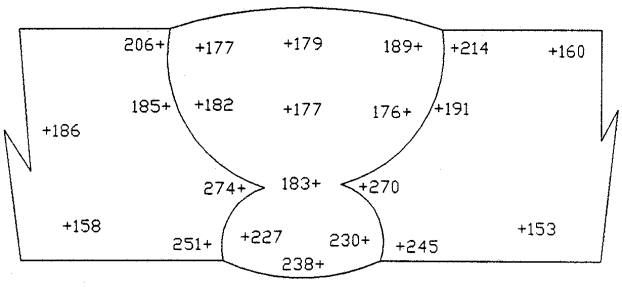

Fig. 9 Hardness profile across the weld joint

3.5 Weld Joint Configurations

Welding of ASTM A 537 Cl. 1 plates for pressure vessel and construction applications requires different joint configurations depending upon the thickness of the plate and the welding process employed. Five weld joint configurations, namely single lap joint, double lap joint, angular butt joint, cruciform fillet joints with edge preparation, and cruciform fillet joint without edge preparation were prepared (Fig. 10) using the SMAW process. The results of tensile shear tests carried out on the five joint types are presented in Table 5. All the five weld joints meet the minimum specified tensile strength level for ASTM A 537 Cl. 1 steel (50.0 kg mm^{-2}).

It is evident on the basis of various tests conducted in the present study that the weld joint possesses adequate internal soundness and exhibits an excellent combination of strength and toughness properties. Based on the above results, a recommended welding procedure for this grade of steel was formulated.

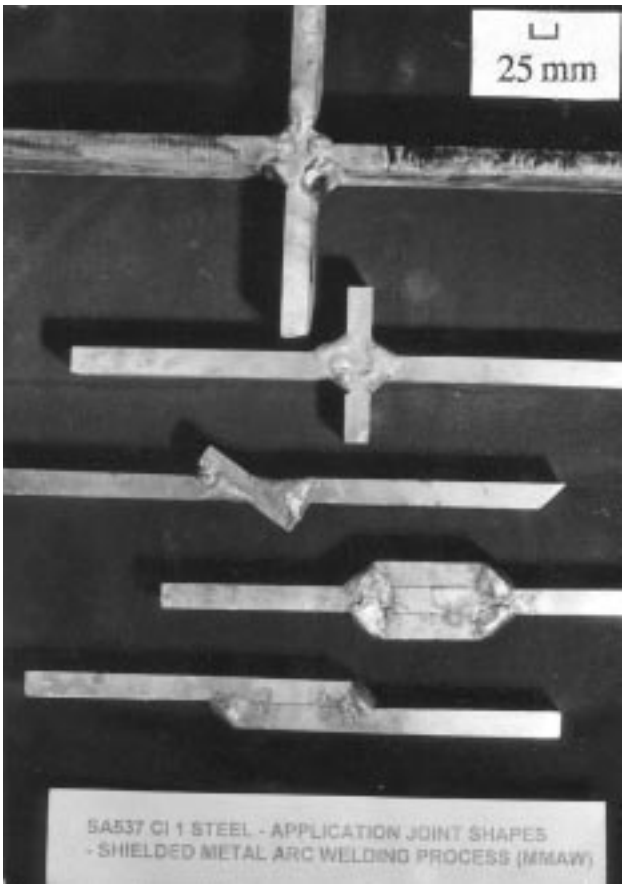

Fig. 10 Different types of weld joint configurations prepared using the SMAW process

4. Conclusions

- Pressure vessel steel conforming to the ASTM A 537 Cl. 1 specification was developed through the BOF-VAD-concast-plate mill route. The plates possess a good combination of strength-ductility-toughness properties (YS, 36-39 kg mm^{-2}; TS, 58-61 kg mm^{-2}; elongation, 25-28% and CIE, 8-12 kg-m at –20 °C).
- Implant tests carried out using unbaked, partially baked, and fully baked electrodes yielded SFL values of 46.6, 45.8, and 52.0 kg mm^{-2} respectively, in excess of the MSYS (35 kg mm^{-2}), indicating good resistance to cold cracking.
- The critical restraint intensity (K_{cr}) was found to be in excess of 3540 kg/mm^2 under no preheat and partial/full rebake conditions. This is considered adequate for most structural applications where restraint levels (K) vary from 200 to 1640 kg/mm^2.
- Lamellar tearing tests carried out on full-thickness specimens with unbaked/partially baked/fully baked electrodes and a WRL of 42 to 44 kg mm^{-2}, revealed no incidence of cracks, indicating good lamellar tearing resistance of the weld joint. Lamellar tearing was observed in a machined sample where the HAZ corresponded to the centerline segregated zone of the plate. The combination of two factors were responsible for lamellar tearing: a high hydrogen level (unbaked electrode) and a hard phase (bainite) at the weld joint.
- C and Mn were found to have strong tendencies to segregate at the midthickness of the plate. This led to an increase in the pearlite content from a mean value of 40% (matrix) to around 80% at the midthickness (segregated band) of the plate. It also promoted the localized formation of the hard bainitic phase. It was evident from the study that cracks nucleated within these pockets and propagated through the band leading to lamellar tearing.
- The weld zone revealed an acicular ferrite structure with dispersed islands of proeutectoid ferrite at prior austenite grain boundaries. The HAZ revealed a typical bainitic structure. The weld joint was found to possess adequate strength (TS 56.8 kg mm^{-2}) and impact toughness properties (CIE 7.4 and 4.5 kg-m at –20 °C for WM and HAZ, respectively). The CTOD values, determined to be 0.36 mm and 0.27 mm respectively for WM and HAZ, indicated adequate resistance to brittle fracture.
- Results of tensile shear tests conducted on five commonly used joint configurations showed that the weld joints possess adequate internal soundness and meet the MSTS (50.0 kg mm^{-2} min) requirements for ASTM A 537 Cl. 1 steel.

Acknowledgments

The authors are grateful to the management of the R & D Centre, SAIL and the Welding Research Institute, Trichy for their encouragement and support. The authors are especially thankful to Shri K.L. Rohira and Shri R. Veeraraghavan of the Welding Research Institute, Trichy for their help, cooperation, and valuable suggestions during the course of this work.

References

1. R. Datta, S. Mishra, J. Singh, V. Kumar, and S. Kumar, Production of Pressure Vessel Plates, *Steel Techol. Int.*, 1994-95, p 109-112
2. S.K. Chaudhuri, R. Datta, A.K. De, and S. Mishra, Recent Efforts in High Strength Steel Development at SAIL, *Trans. Indian Inst. Met.*, Vol 49 (No. 3), 1996, p 207-216
3. M.J. Cieslak, Cracking Phenomona Associated with Welding, *Welding, Brazing, and Soldering,* Vol 6, *ASM Handbook*, ASM International, 1993, p 88-96
4. H. Granjon, *Fundamentals of Welding Metallurgy,* Abington Publishing, 1991, p 156
5. *Metals and Weldability, AWS Welding Handbook,* 7th ed., 1984
6. F.R. Coe, Welding Steels Without Hydrogen Cracking, *Fundamentals of Welding Metallurgy,* Abington Publishing, 1973, p 24-39
7. International Institute of Welding (IIW) Doc. 830-73, 1973
8. S. Myoshi, Influence of Operating Conditions and Mechanical Factors on Centre Segregation of Slabs, *Proc. Continuous Casting of Steel,* The Metals Society/IRSID, 1976, p 286-291
9. C.J. Van Vuuren, Operating and Quality Control Aspects of the Production of Critical Low and High Carbon Products from Continuously Cast Blooms, *Steelmaking Proceedings,* Iron & Steel Society, Warrendale, Vol 61, 1978, p 306-334